PNAS
www.pnas.org

Supplementary Information for

Bifurcation of excited state trajectories towards energy transfer or electron transfer directed by wavefunction symmetry

Paola S. Oviedo, Luis M. Baraldo, Alejandro Cadranel.

Alejandro Cadranel
Email: acadranel@qi.fcen.uba.ar
Luis M Baraldo
Email: baraldo@qi.fcen.uba.ar

This PDF file includes:

UV-vis absorption spectra and spectroelectrochemistry of RuRuCr and $RuCr^-$

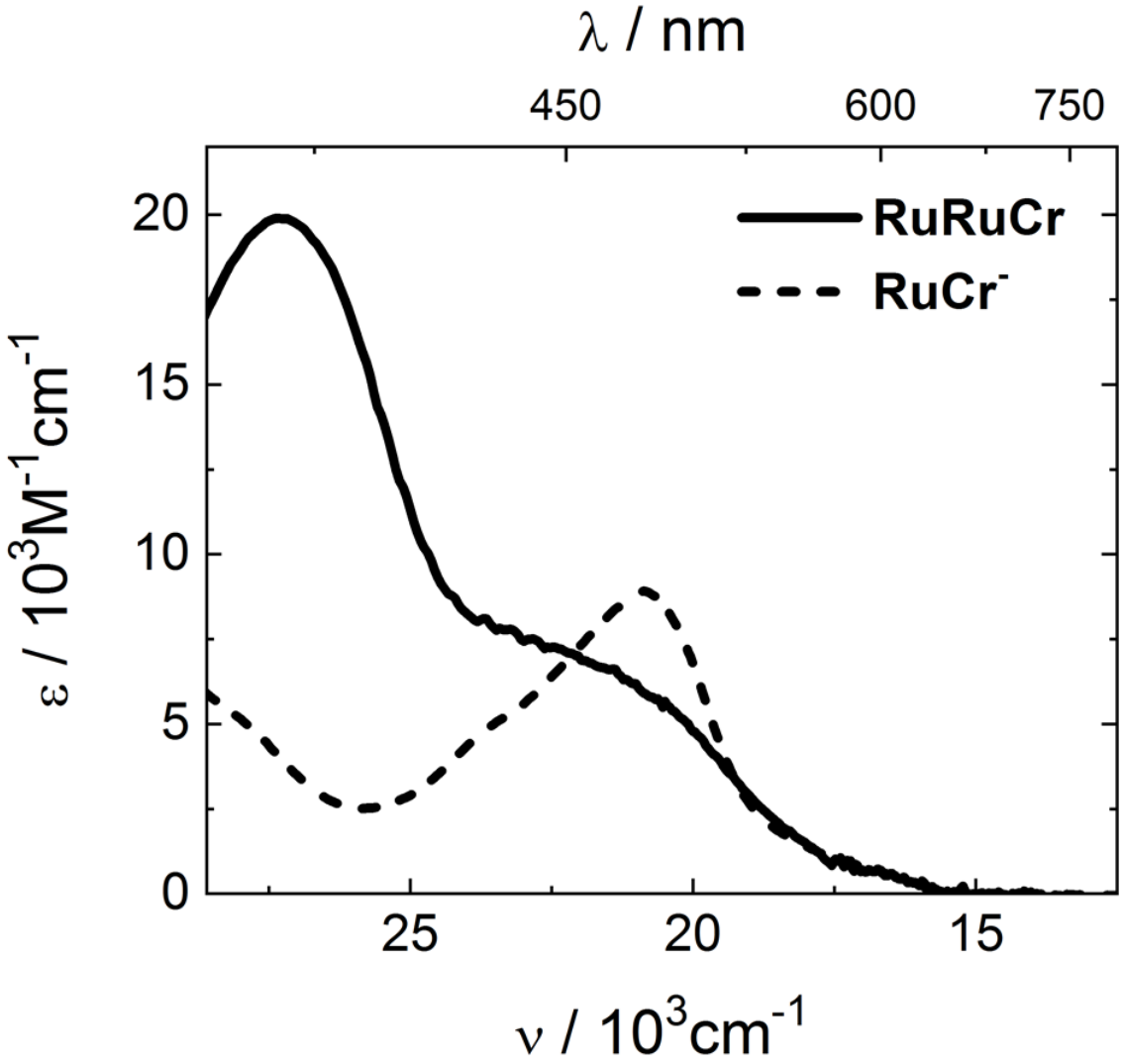

Fig. S1. Absorption spectra of RuRuCr and $RuCr^-$ in DMSO at room temperature.

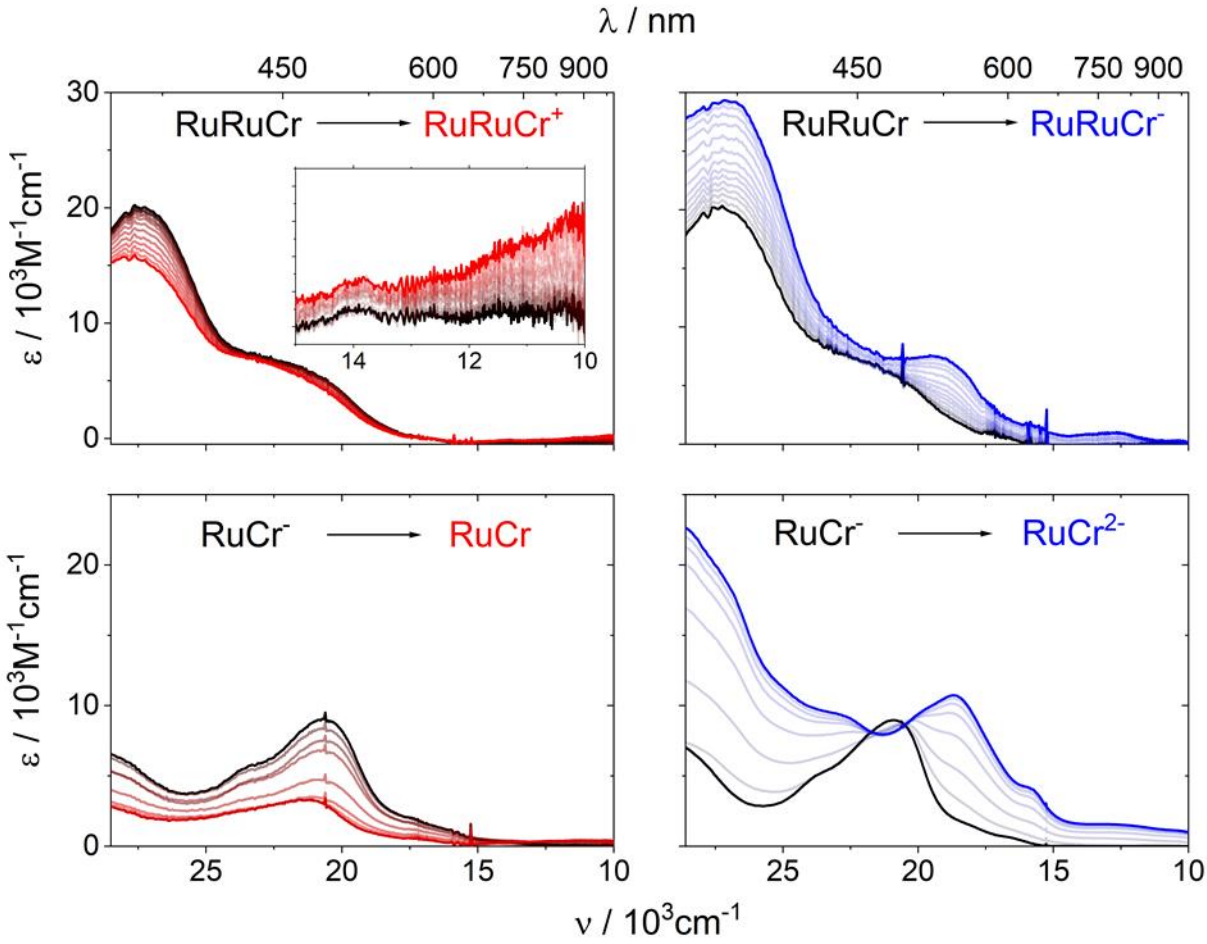

Fig. S2. Evolution of the absorption spectra upon one electron oxidation (left) and one electron reduction (right) of RuRuCr in DMSO (top) and $RuCr^-$ in ACN (bottom) at room temperature. Spectra of the original (black), oxidized (red) and reduced (blue) species are shown.

nsTAS of RuRuCr in DMSO

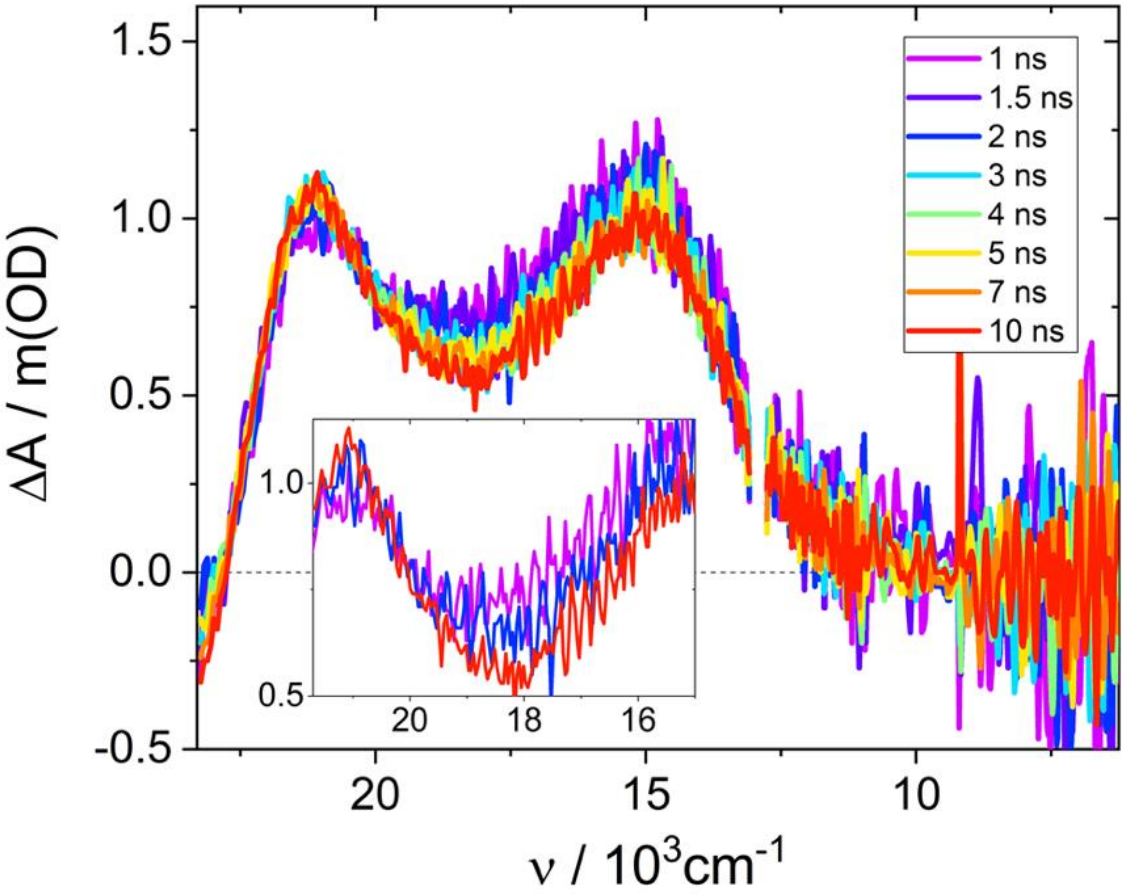

Fig. S3. nsTA spectra of RuRuCr at selected time delays in DMSO at room temperature, under 25800 cm^{-1} (387 nm) excitation.

Table S1. Transient absorption spectroscopy data obtained upon target analysis of RuRuCr and $RuCr^-$.

			fsTAS				**nsTAS**	
		ν_{ex} / $10^3 cm^{-1}$	**^{3}MLCTr / hot-^{3}MLCT**	**^{3}MLCTz**	**^{3}MLCTxy**	**^{2}E**	**^{3}MLCTxy**	**^{2}E**
			τ / ps k / ps^{-1}	**τ / ps k / ps^{-1}**	**τ / ns k / ns^{-1}**	**τ / μs k / μs^{-1}**	**τ / ns k / ns^{-1}**	**τ / μs k / μs^{-1}**
RuRuCr	DMSO	25.8	6 (0.164 ±0.007)	106 (9.40 ±0.15)	0.95 (1.044 ±0.002)	n.r.	4.4 (0.23 ±0.04)	13.1 (0.08 ±0.02)
		19.8	1.5 (0.632 ±0.003)	110 (9.1 ±0.1)	1.50 (0.67 ±0.02)	n.r.	-	-
$RuCr^-$	DMSO	19.8	n.o.	5.2 (0.1913 ±0.0002)	n.r.		8.3 (0.121 ± 0.003)	17.4 (0.05742 ± 0.00006)
	H_2O	19.8	n.o.	5.2 (0.1911 ±0.0002)	0.95 (0.10535 ± 0.00007)	n.r.	n.r.	0.376 (2.658 ± 0.003)

n.r.: not resolved due to timescale constraints. n.o.: not observed.

nsTAS of $RuCr^-$ in DMSO

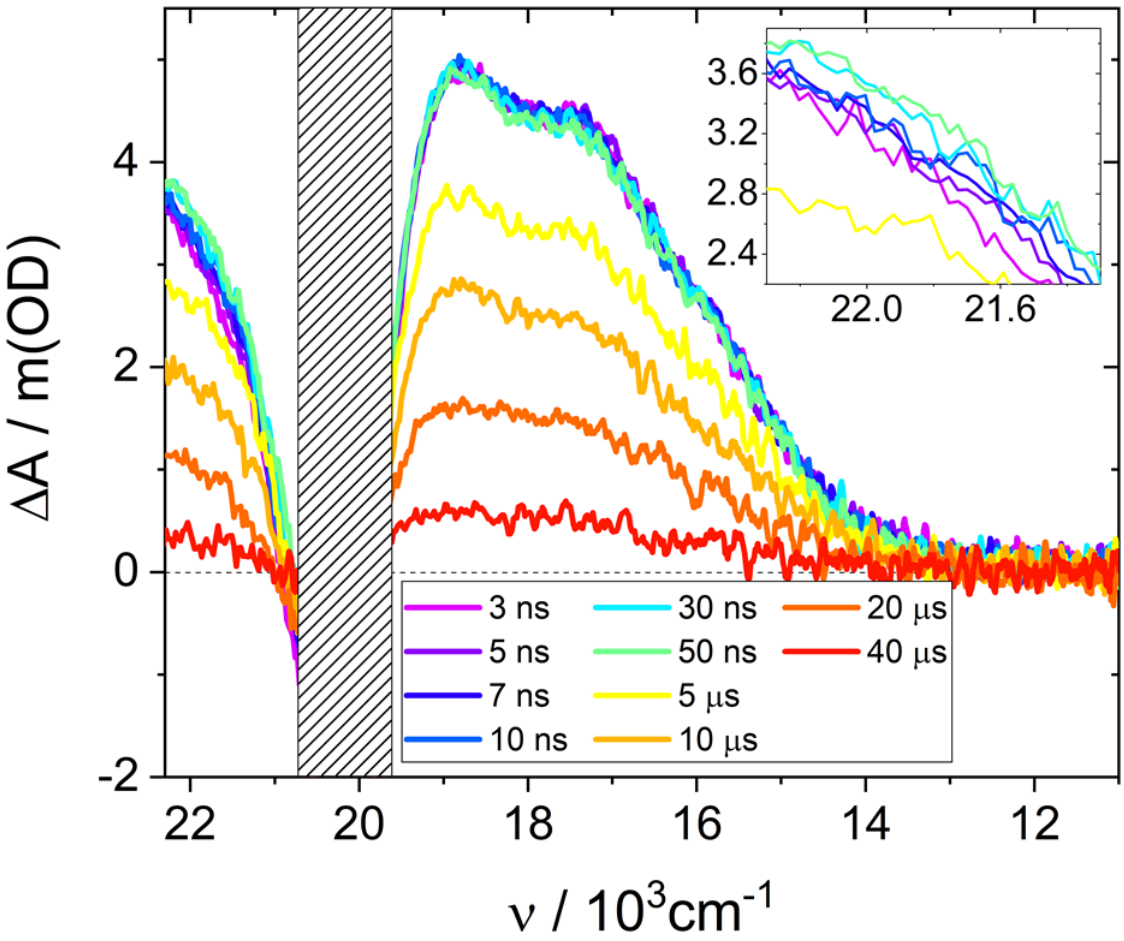

Fig. S4. nsTA spectra of $RuCr^-$ in DMSO at room temperature, under 25800 cm^{-1} (505 nm) excitation.

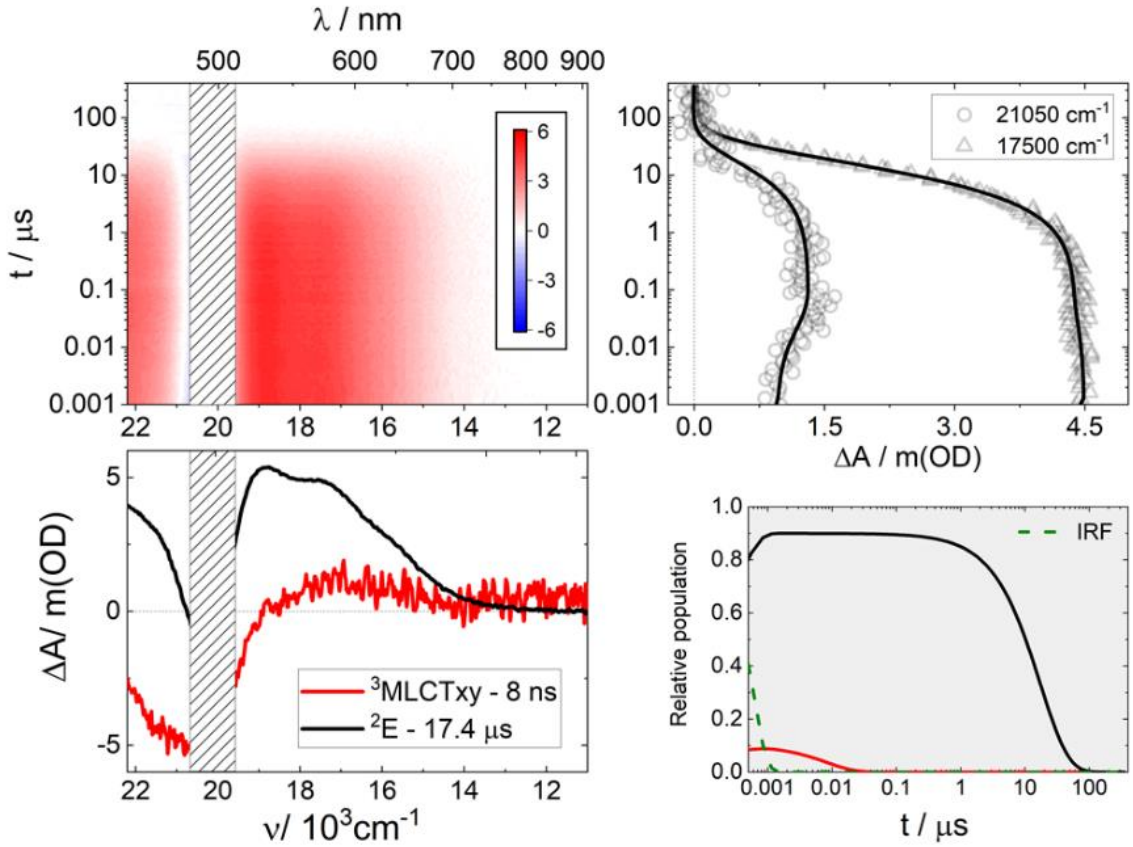

Fig. S5. Differential absorption 3D map obtained from nsTAS with 19800 cm^{-1} (505 nm) excitation of $RuCr^{-}$ in DMSO at room temperature (upper left). Species associated differential spectra of **^{3}MLCTxy** and **^{2}E(Cr)** (bottom left). Differential absorption kinetic traces at 17500 and 21050 cm^{-1} (upper right), and relative populations of **^{3}MLCTxy** and **^{2}E(Cr)** (bottom right).

fsTAS of RuRuCr in DMSO

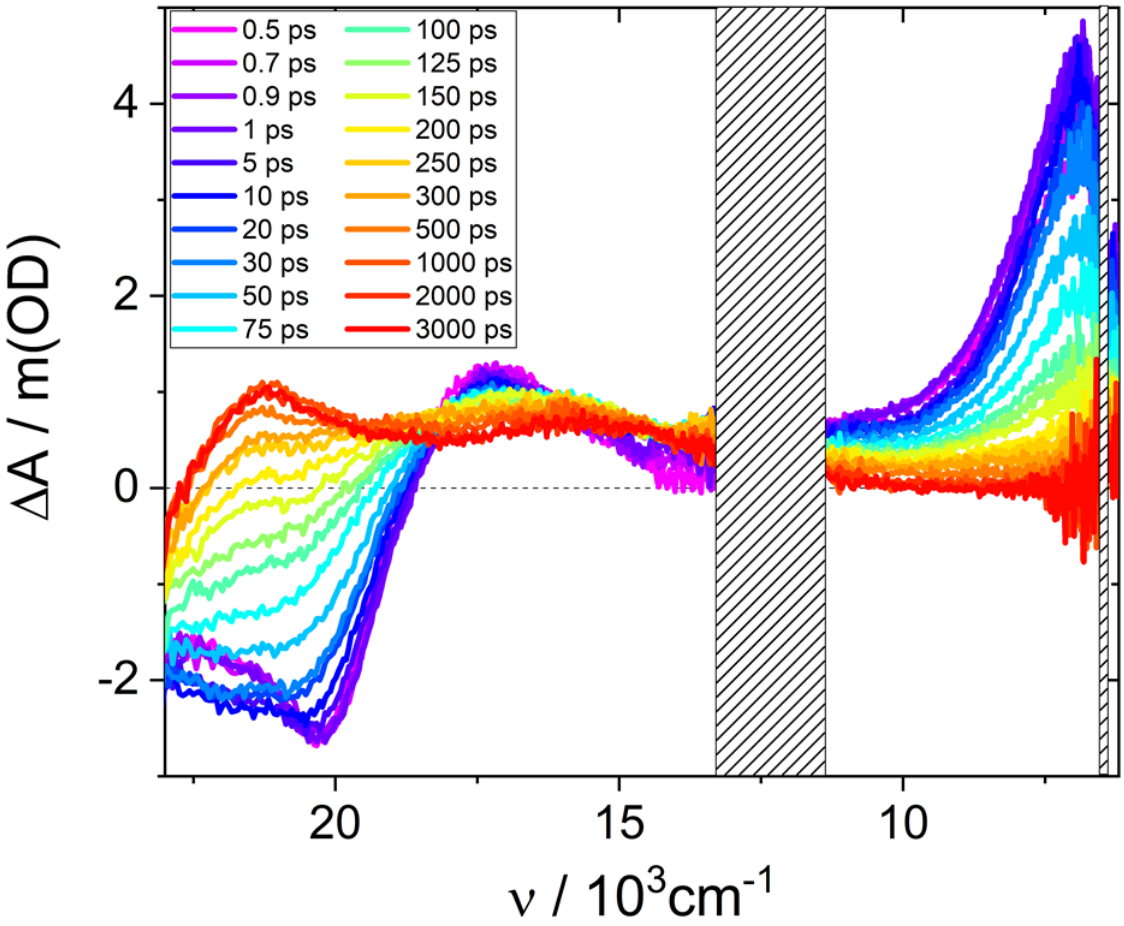

Fig. S6. fsTA spectra of RuRuCr at selected time delays in DMSO at room temperature, under 25800 cm^{-1} (387 nm) excitation.

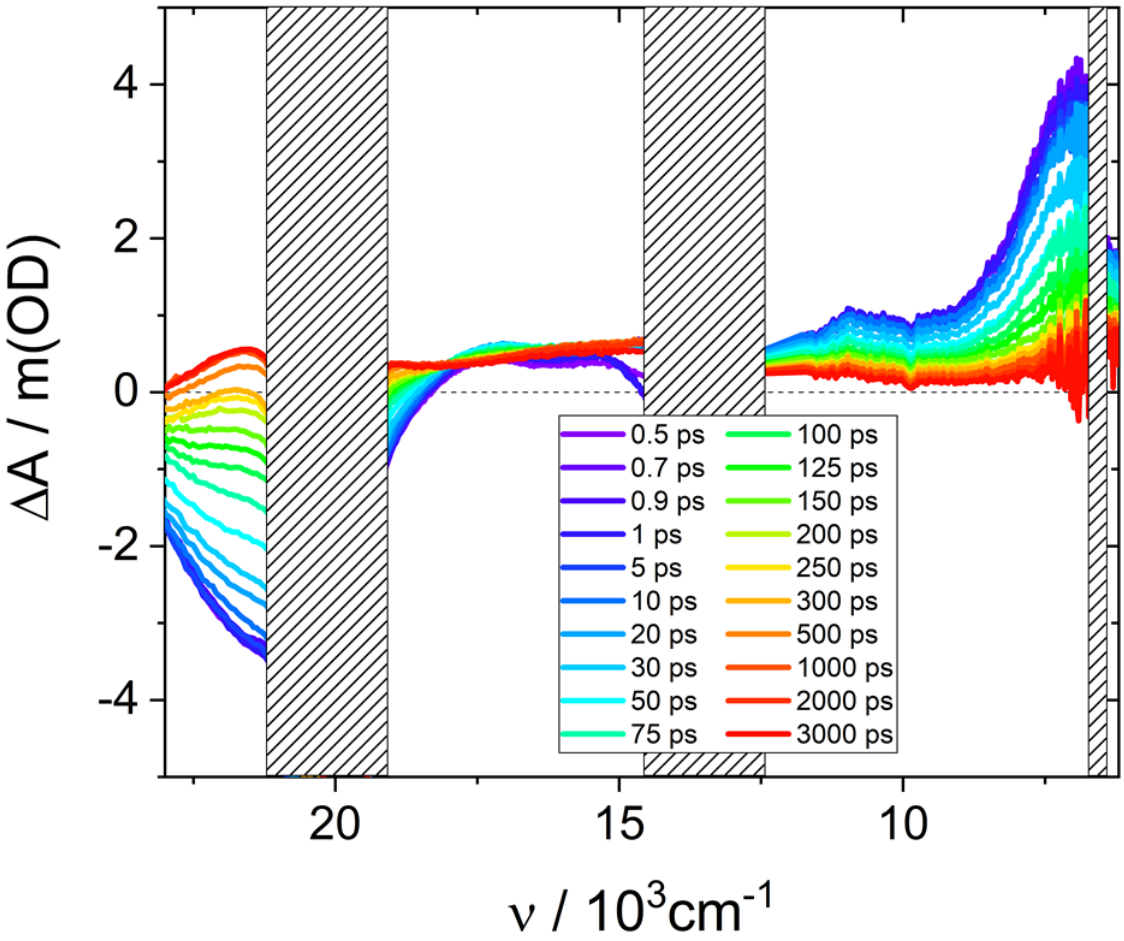

Fig. S7. fsTA spectra of RuRuCr at selected time delays in DMSO at room temperature, under 19800 cm^{-1} (505 nm) excitation.

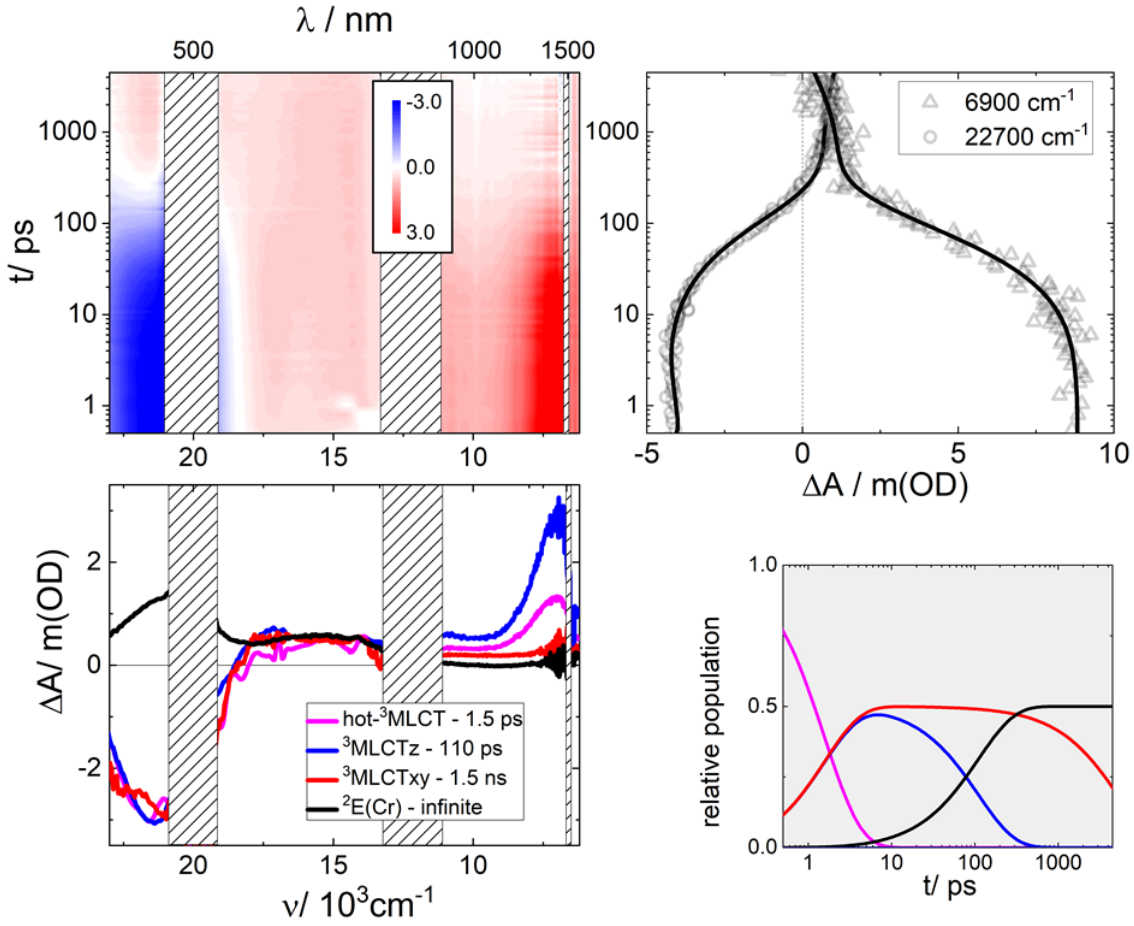

Fig. S8. Differential absorption 3D map obtained from fsTAS with 19800 cm^{-1} (505 nm) excitation of RuRuCr in DMSO at room temperature (upper left). Species associated differential spectra of **hot-^{3}MLCT**, **^{3}MLCTz** , **^{3}MLCTxy** and **^{2}E(Cr)** (bottom left). Differential absorption kinetic traces at 6900 and 22700 cm^{-1} (upper right), and relative populations of **hot-^{3}MLCT**, **^{3}MLCTz** , **^{3}MLCTxy** and **^{2}E(Cr)** (bottom right).

fsTAS of $RuCr^-$ in DMSO

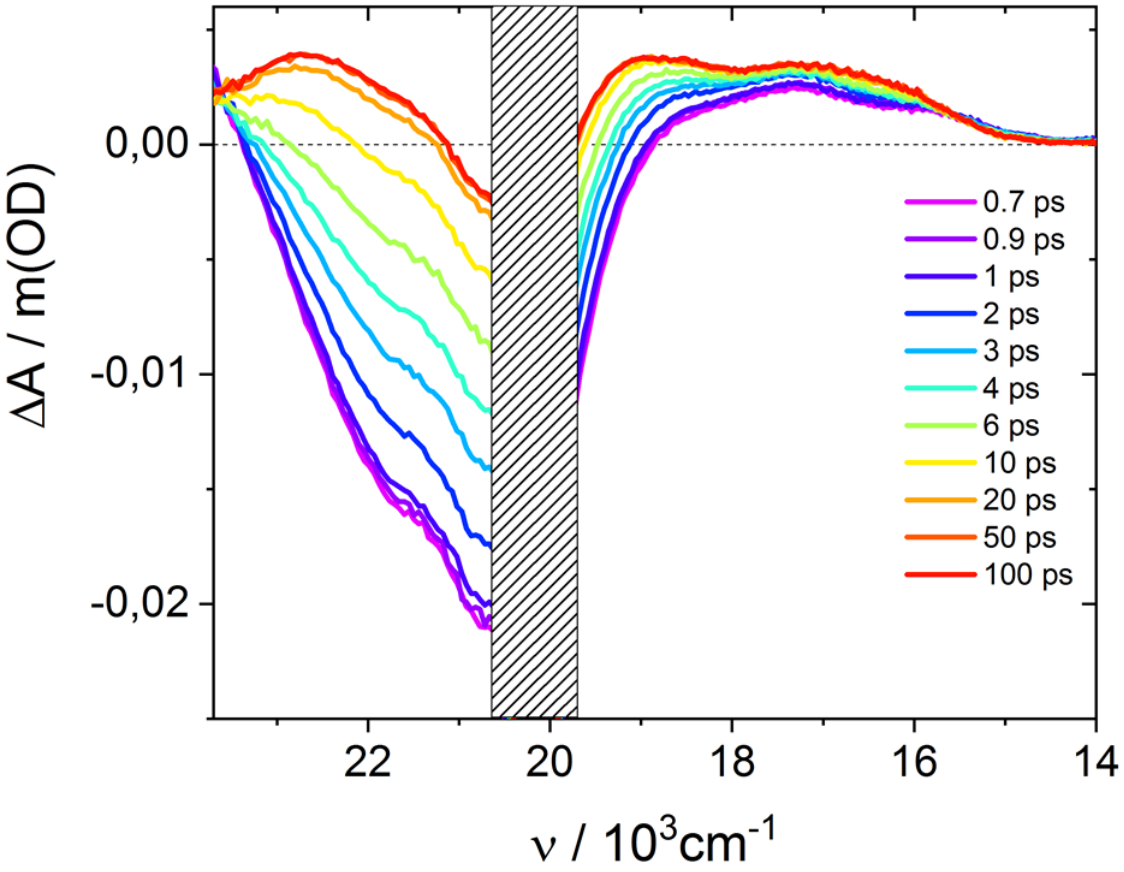

Fig. S9. fsTA spectra of $RuCr^-$ at selected time delays in DMSO at room temperature, under 19800 cm^{-1} (505 nm) excitation.

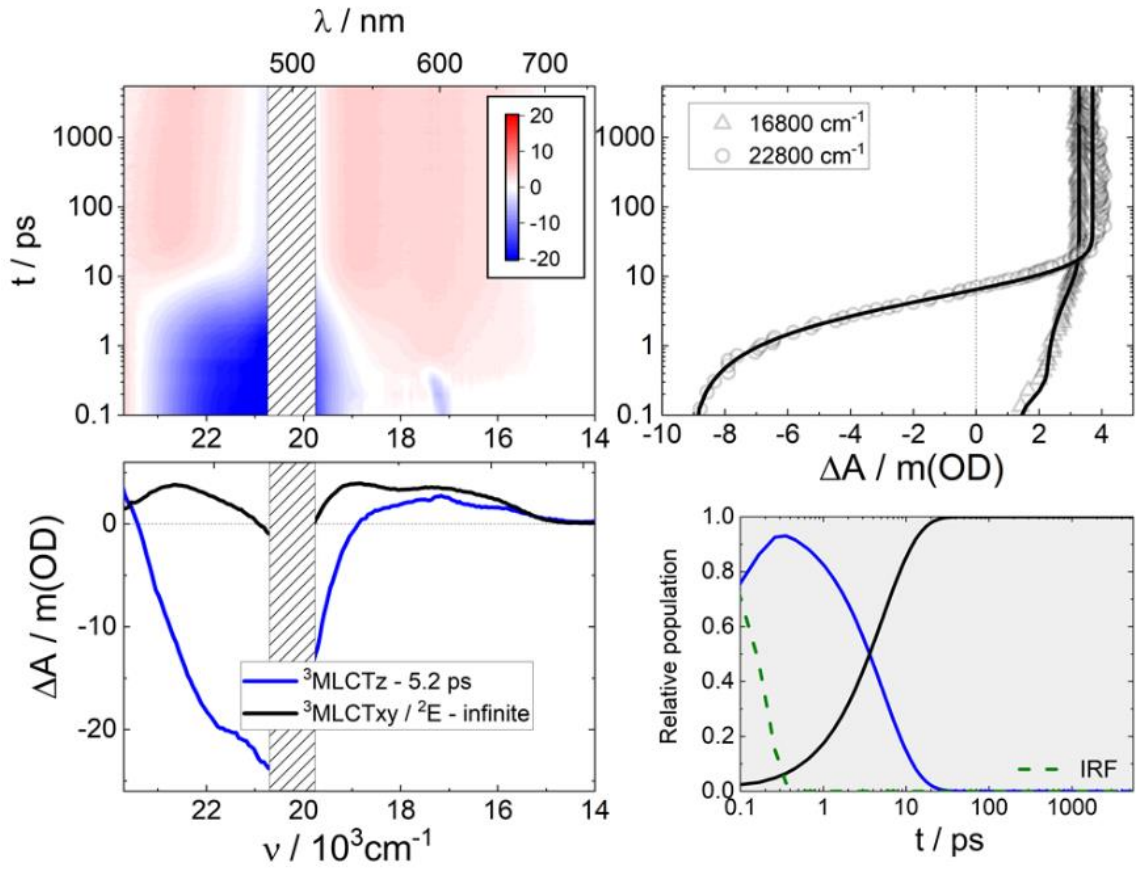

Fig. S10. Differential absorption 3D map obtained from fsTAS with 19800 cm^{-1} (505 nm) excitation of $RuCr^{-}$ in DMSO at room temperature (upper left). Species associated differential spectra of **^{3}MLCTz** and **^{3}MLCTxy / ^{2}E(Cr)** (bottom left). Differential absorption kinetic traces at 16800 and 22800 cm^{-1} (upper right), and relative populations of **^{3}MLCTz** and **^{3}MLCTxy / ^{2}E(Cr)** (bottom right).

Target model for $RuCr^{-}$

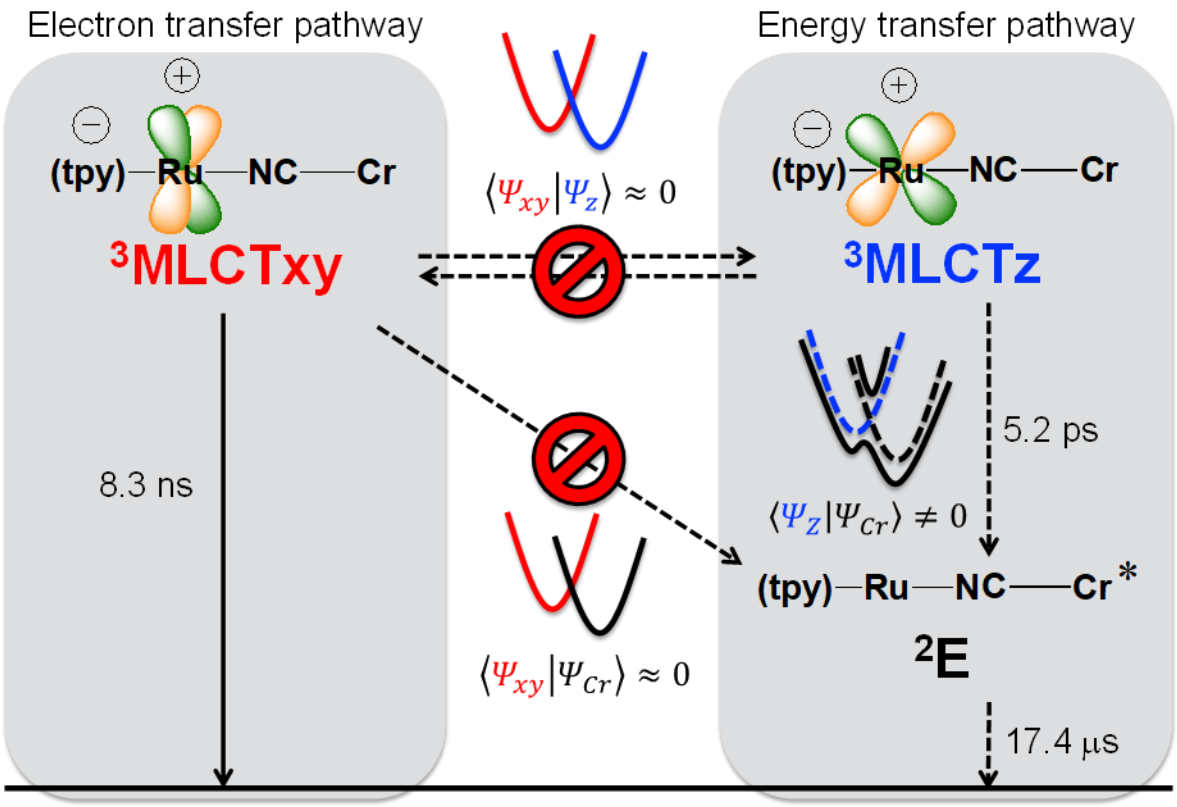

Fig. S11. Target model applied to fit the transient absorption data, considering separate electron transfer and energy transfer pathways for $RuCr^{-}$. Electronic coupling between states of different wavefunction symmetry is small and results in two separate reaction pathways.

Results using target models for RuRuCr and $RuCr^{-}$ considering that ^{3}MLCTxy feeds ^{2}E

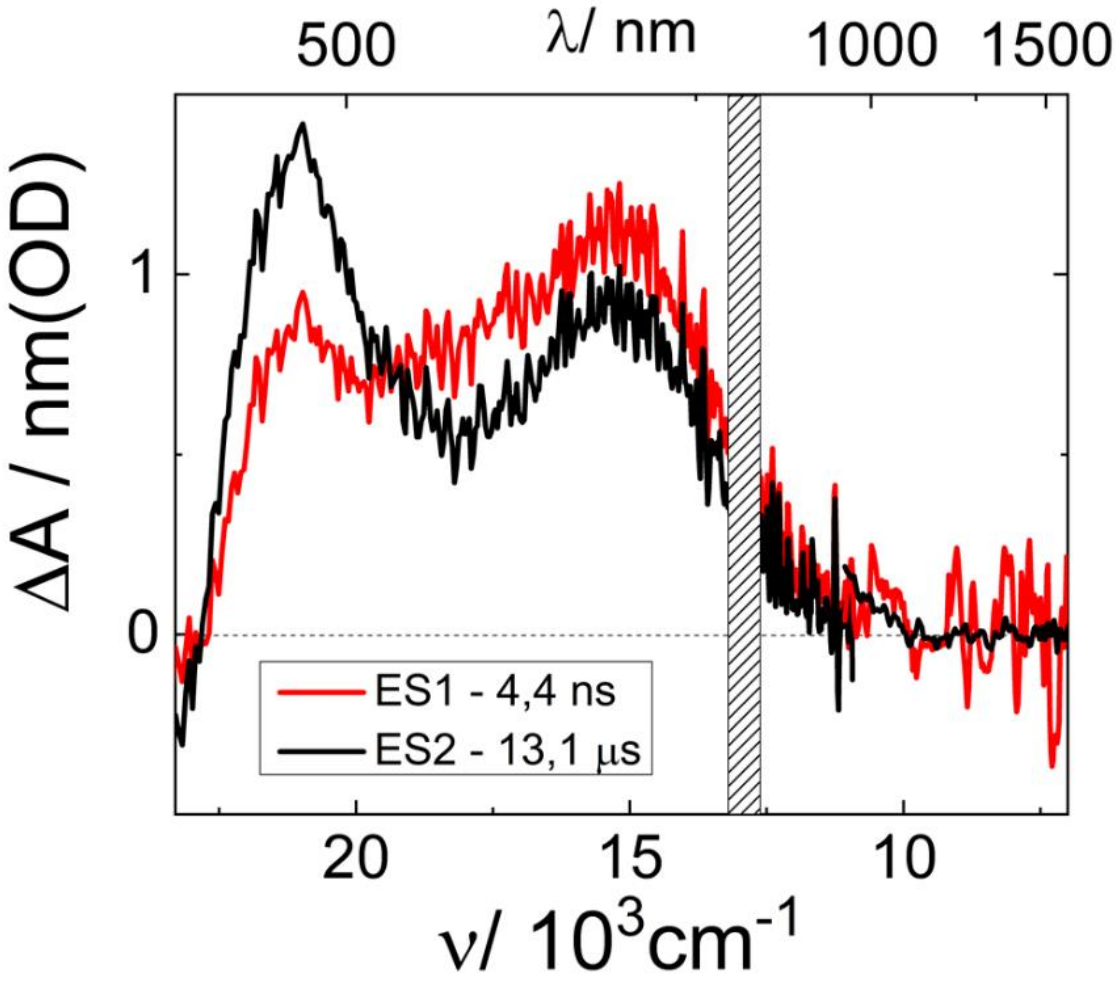

Fig. S12. Decay associated spectra obtained from global analysis of nsTAS data for RuRuCr in DMSO at room temperature, under 25800 cm^{-1} (387 nm) excitation.

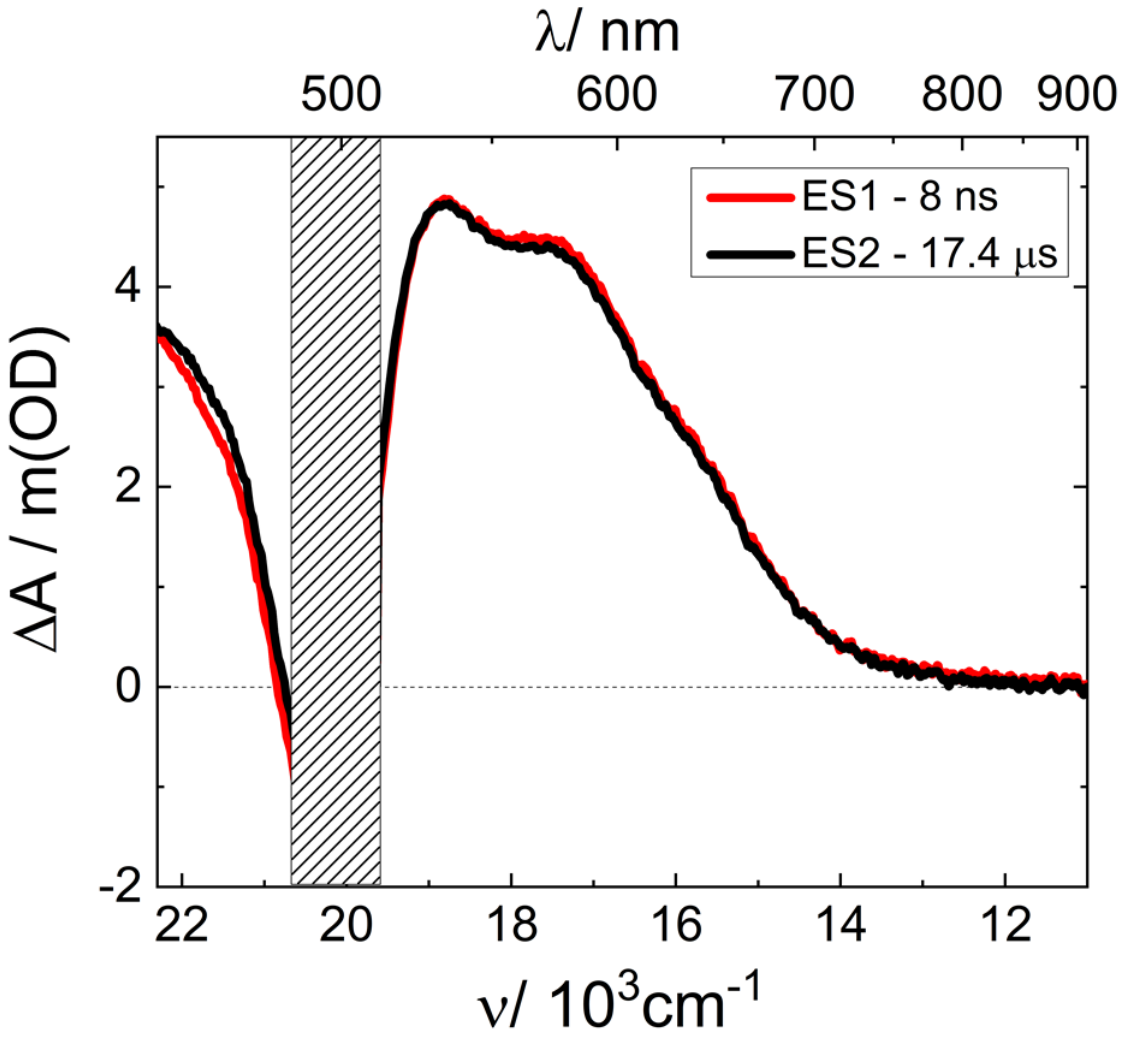

Fig. S13. Decay associated spectra obtained from global analysis of nsTAS data for $RuCr^{-}$ in DMSO at room temperature, under 19800 cm^{-1} (505 nm) excitation.

Photolysis experiments of RuRuCr and $RuCr^-$ in DMSO

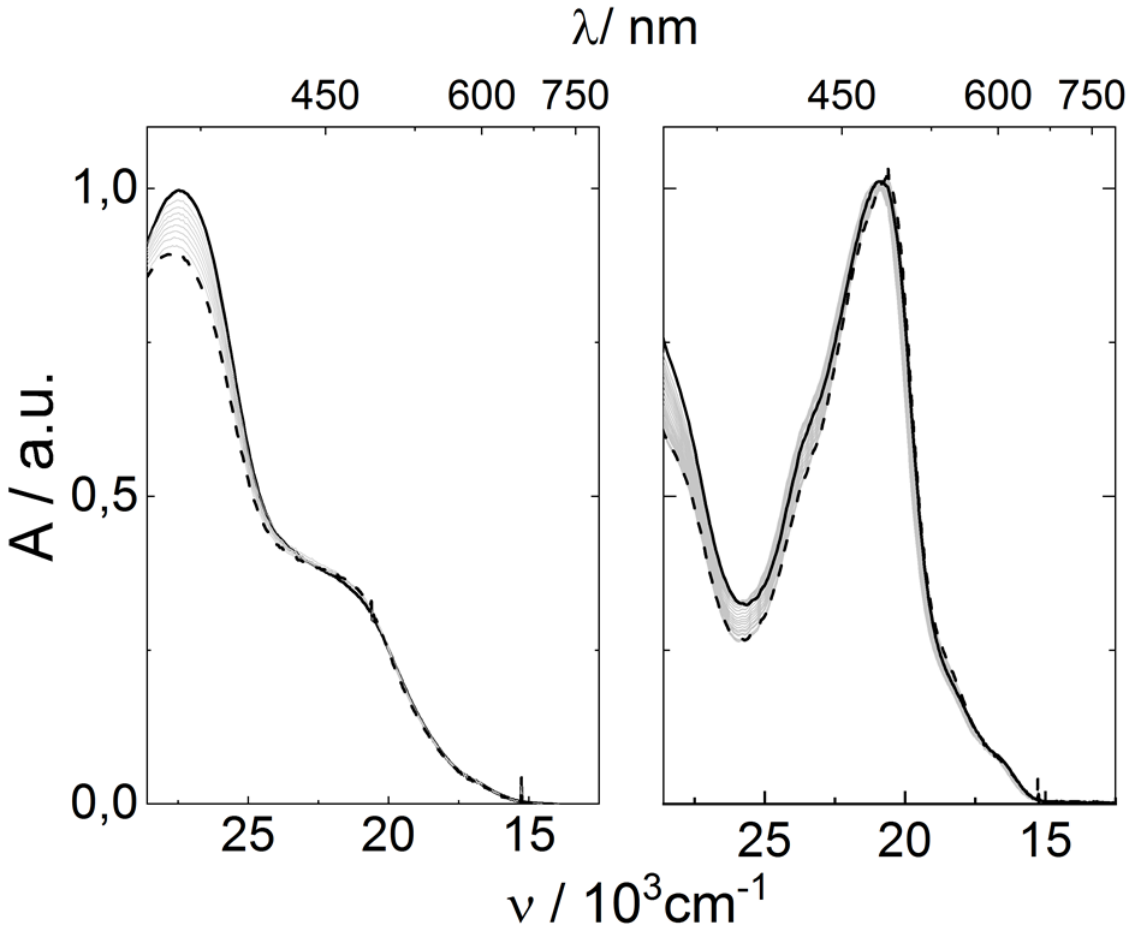

.

Fig. S14. Evolution of the absorption spectra of RuRuCr (left) and $RuCr^-$ (right) upon 4 hour illumination at 450 nm.

nsTAS and fsTAS of $RuCr^-$ in H_2O

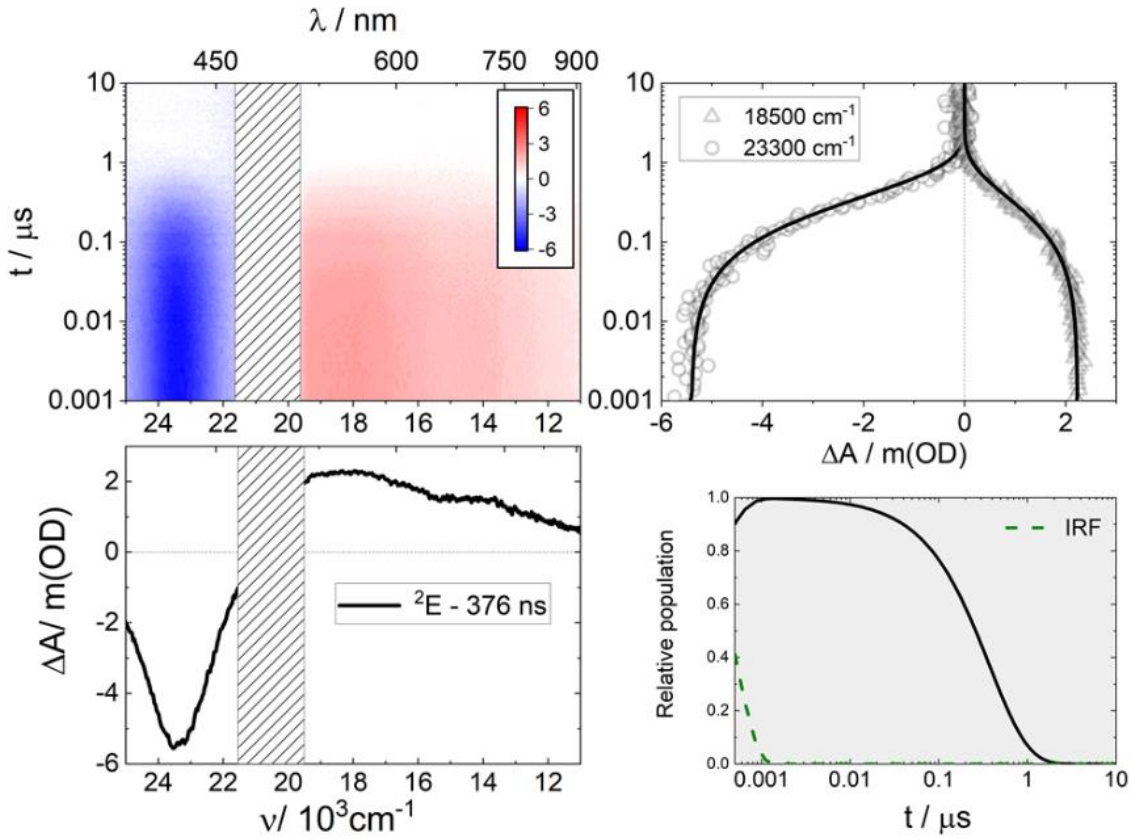

Fig. S15. Differential absorption 3D map obtained from nsTAS with 19800 cm^{-1} (505 nm) excitation of $RuCr^-$ in H_2O at room temperature (upper left). Species associated differential spectra of **^{2}E(Cr)** (bottom left). Differential absorption kinetic traces at 18500 and 23300 cm^{-1} (upper right), and relative populations of **^{2}E(Cr)** (bottom right).

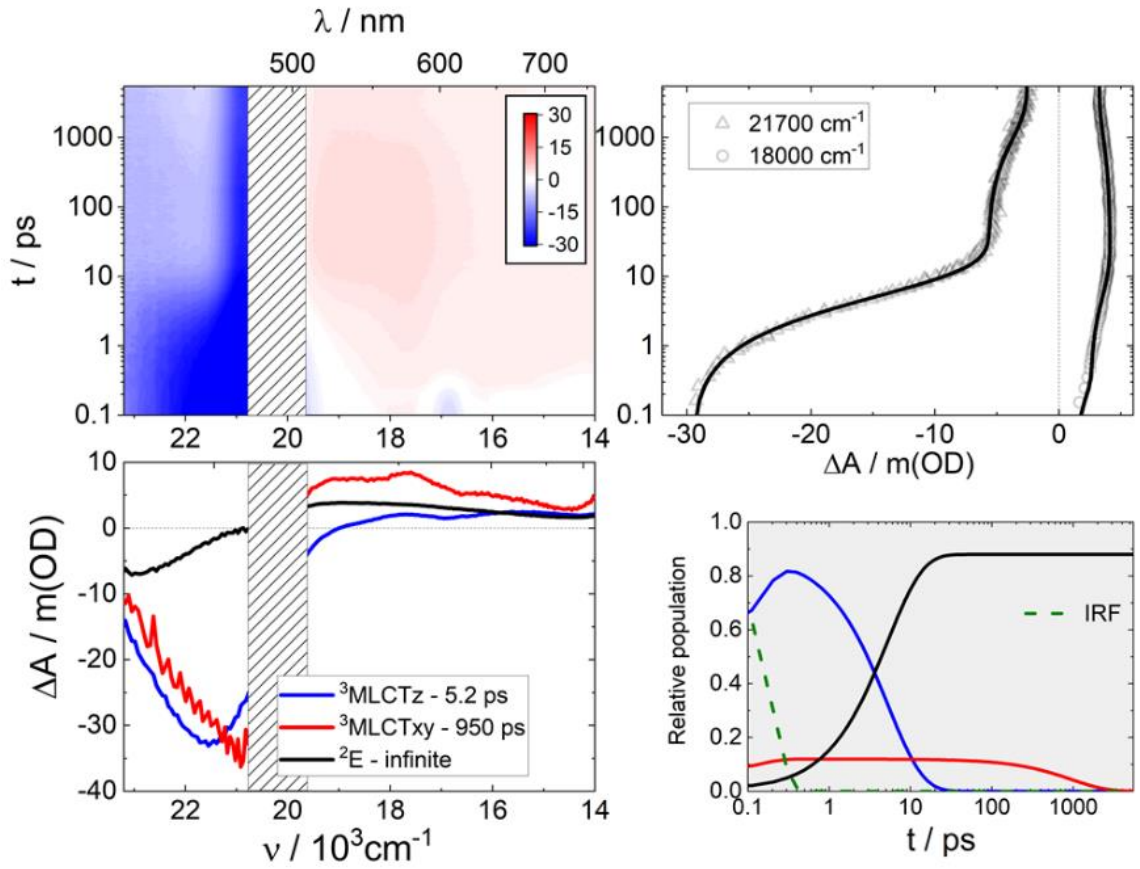

Fig. S16. Differential absorption 3D map obtained from fsTAS with 19800 cm^{-1} (505 nm) excitation of $RuCr^{-}$ in H_2O at room temperature (upper left). Species associated differential spectra of **^{3}MLCTz** , **^{3}MLCTxy** and **^{2}E(Cr)** (bottom left). Differential absorption kinetic traces at 18000 and 21700 cm^{-1} (upper right), and relative populations of **^{3}MLCTz** , **^{3}MLCTxy** and **^{2}E(Cr)** (bottom right).